DIODE LASER SPECTROSCOPY

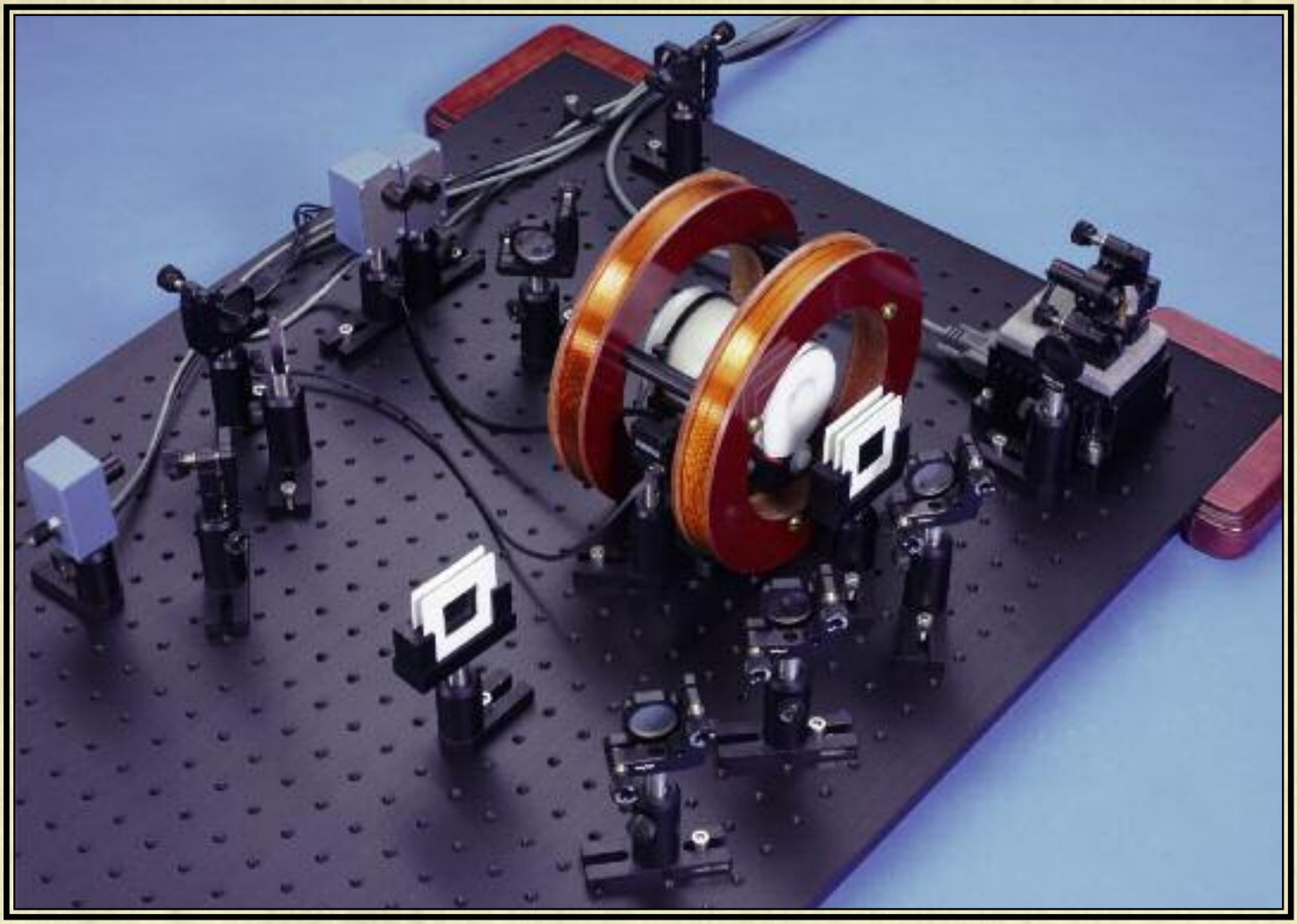

Spectroscopy, and Much More, Using Modern Optics

- Observe Doppler-Free Spectroscopy of Rubidium Gas
- Michelson Interferometer Used to Calibrate Laser Sweep
- Observe Resonant Faraday Rotation in Rb Vapor
- Measure Temperature Dependence of Absorption and Dispersion Coefficients of Rb Vapor
- Lock Laser to Rubidium Hyperfine Transition
- Study Zeeman Splitting in Rb Spectrum at Two Wavelengths
- Study Stabilized Diode Laser Characteristics

Instruments Designed For Teaching

TEACH SPIN

DIODE LASER SPECTROSCOPY

INTRODUCTION

Spectroscopy can be broadly defined as the study of the interaction of electromagnetic radiation with matter. Since its discovery, it has been a cornerstone of experimental and theoretical physics. Originally, spectroscopy was confined to examining the interaction of visible light with gases. With the development of quantum mechanics, spectroscopy took center stage in verifying the predictions of this radical theory.

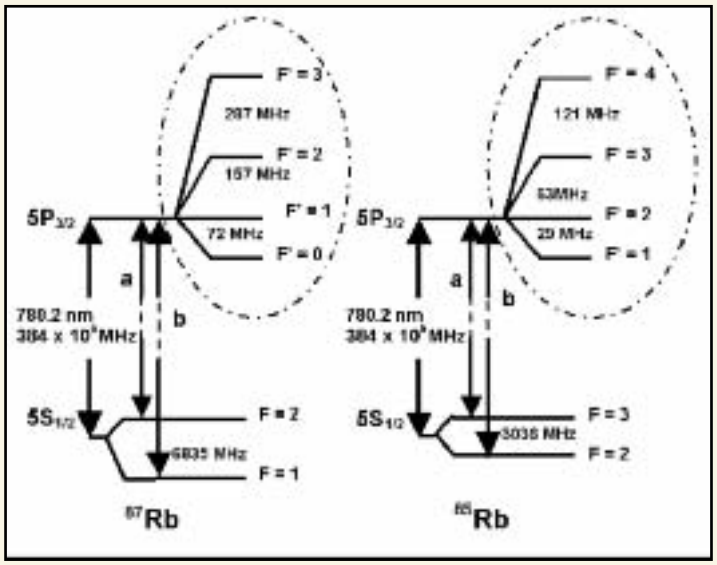

Fig. 1: Rubidium Atomic Energy Level Diagrams

However, there appeared to be a intrinsic limit to the precision of a spectroscopic measurement of gases. This arises from the motion of the atoms in any gas, which Doppler-broadens both the absorption and emission lines of the spectrum. For a typical gas at room temperature, this broadening is $\Delta\upsilon_{Dopp} \sim 1$ GHz whereas the lifetime-limited linewidth of the rubidium D line is about 6 MHz, a factor of 200 smaller.

This limitation was cleverly bridged by the discovery of Doppler-free (D-F) spectroscopy. These experiments still study atoms in the gaseous state, but ingeniously select out the atoms with zero velocity component along one direction. The essential component of the new Doppler-free spectroscopy was the tunable laser light source. The very first lasers were hardly tunable, but by the mid 1960's tunable dye lasers were being used for pioneering atomic physics experiments. These lasers required a fixed frequency, high-power laser pump and a chemical dye stream that produced the laser emission. These light sources were large, cumbersome, and expensive to purchase and to maintain, putting them far outside the range of the teaching laboratory.

The more recent development of tunable narrow-bandwidth semiconductor diode lasers dramatically changed this picture. These lasers are inexpensive, easy to operate, and produce high power, tunable, narrow-bandwidth radiation ($\Delta\upsilon \sim 1$ MHz).

TeachSpin, in collaboration with Professor Kenneth Libbrecht of the California Institute of Technology, has produced the first tunable, stabilized, diode laser system specifically designed for the advanced laboratory. Finally, an affordable, student-friendly, diode laser apparatus which does "spectroscopy and much more" is available for exploring atomic physics!

APPARATUS

The centerpiece of the apparatus is the grating-stabilized diode laser. Honed to research quality by our senior scientist, George Herold, the laser is both temperature and current regulated. Optical feedback from a grating, retroreflects laser light to create an external cavity that stabilizes the laser to run at a controllable wavelength. A piezo stack, mounted in the grating support, allows the grating position to be modulated by an applied voltage. Using the internal ramp generator to modulate both the laser current and piezo stack, students readily achieve laser sweeps of 10 GHz.

Fig. 2: The Diode Laser Head

Figure 7 shows the modular controller. The modules can be interrogated independently, encouraging exploration of the effects of changing a wide variety of parameters. Students turn dials to control the laser current and temperature, the Rb cell temperature, the piezo stack, and the ramp generator. Signals from two detectors can be balanced, differenced, and amplified. Low-pass and DC level controls can be used to side-lock the laser.

The Rb vapor cell is enclosed in a special temperature controlled oven. Although electrically heated, it produces no measurable ac or dc magnetic field at the sample. The heater is designed to keep the end windows of the cell free from condensing rubidium metal. A cold finger, attached to the middle of the cell, provides the rubidium reservoir. The oven also provides a clear side window for observing the rubidium fluorescence with the CCD camera. A Helmholtz pair of coils surrounds the cell producing a 10 mT magnetic field along the optical path with a current of 3 amperes. A separate power supply is required to provide this current.

STUDENT EXPERIMENTS

Diode Laser Characteristics

Students can begin these labs by studying the laser itself. Without the grating feedback, they can examine both the threshold current for lasing and the wavelength as a function of laser temperature. The wavelength can be measured with either a homemade spectrometer or any commercial spectrometer already on hand. Students can also observe mode hopping in the laser.

With the grating feedback in place, students can observe the laser's wavelength stability, the frequency sweep (using both grating position and current modulation), and the sweep interruptions due to mode hopping.

Classic Laser Spectroscopy

The simplest form of optical spectroscopy, transmission spectroscopy, is shown in Figure 3.

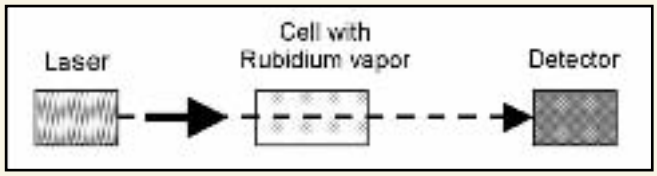

Fig. 3: Block Diagram for Transmission Spectroscopy

The frequency-swept laser light is passed through a cell containing rubidium vapor and the transmitted light is detected. Data for natural rubidium is shown in Figure 4.

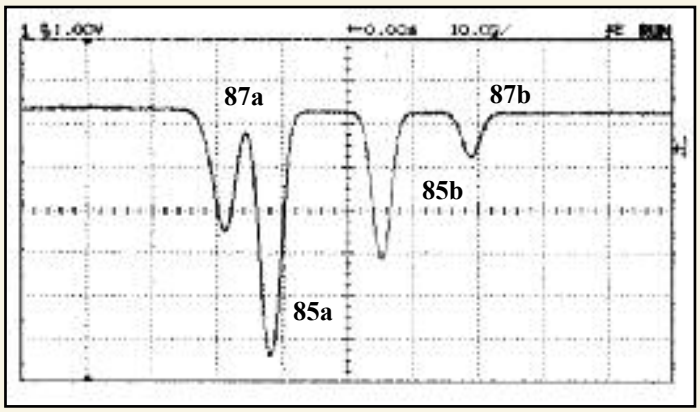

Fig. 4: Transmitted Light vs. Laser Frequency

The broad absorption peaks observed by this method correspond to transitions between the ground $5S_{1/2}$ and the excited $5P_{3/2}$ states of both isotopes of rubidium. These are designated a and b on the energy level diagrams in Figure 1.

A CCD camera connected to a TV monitor is used to observe the infrared fluorescence which occurs when the laser is properly tuned to these transitions. Note that the laser sweep is broad enough to cover both lines of both isotopes. This classic spectroscopic technique easily resolves the ground-state hyperfine splitting of both isotopes, but Doppler broadening obscures the far smaller hyperfine splitting of the exited state.

Doppler-Free Spectroscopy

Now the fun begins. The students rearrange the apparatus so that the single laser beam is split into two co-linear beams, a probe (weak) and a pump (strong), which are sent through the rubidium cell in opposite directions. Figure 5 shows a block diagram of the optical configuration and the front cover is a photograph of this setup. Only the probe beam and a second reference probe beam are detected. For most frequencies within the Doppler range, the pump and probe beams interact with groups of atoms moving with different velocities, so the pump beam has no effect on the transmitted intensity of the probe.

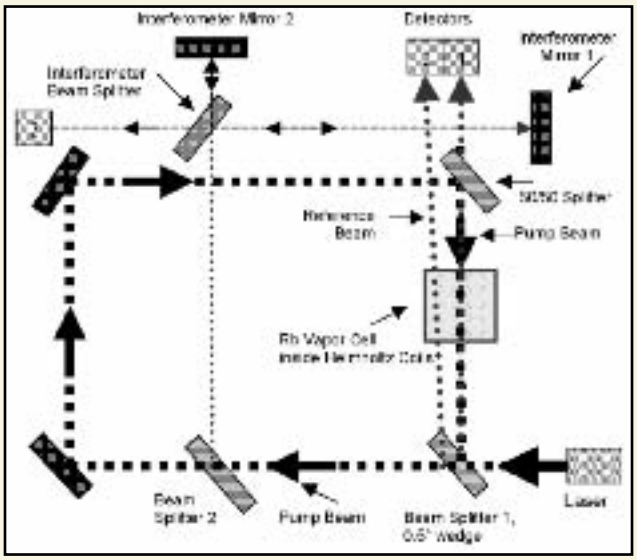

Fig. 5: Block Diagram of D-F and Interferometry

As the laser sweeps through an actual transition frequency, both pump and probe beams interact with the atoms having zero longitudinal velocity. Because the much stronger pump beam "saturates" the transitions, the intensity of the probe beam light reaching Detector 1 increases, producing the narrow features shown in Figure 6.

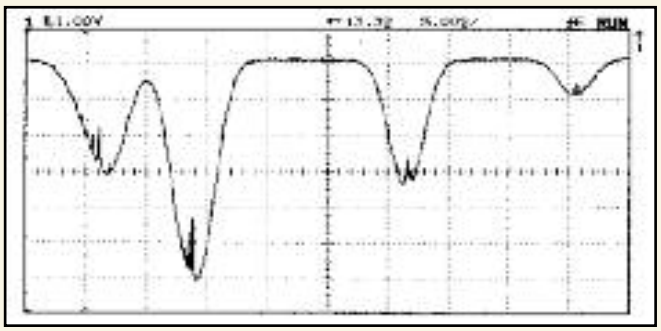

Fig. 6: Narrow Features Indicate $5P_{3/2}$ Hyperfine Structure

Reflection at the second interface of beam splitter 1 produces the *reference beam* which does not overlap the pump beam as it passes through the vapor on its way to Detector 2. The electronics of the controller allows us to subtract this reference beam from the probe beam, removing the Doppler background and leaving only the narrow features. Figure 8 shows this result dramatically for the ground state F=2 transition (a) of ^{85}Rb. With linewidths of about 10 MHz, these features represent a resolution ($\Delta f/f$) of about one part in forty million!

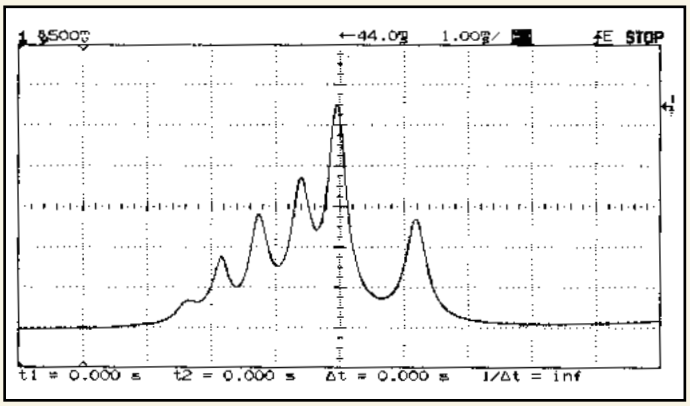

Fig. 8: Features with Doppler Background Removed

Given the $\Delta F = 0, \pm 1$ selection rules, the energy level diagram of ^{85}Rb (Fig. 5), implies that there should be only *three*, not six, transitions from F = 2. The six peaks seen Fig. 8 include three additional *cross-over resonance* peaks. These additional peaks, at frequencies exactly halfway between pairs of "actual" transition frequencies, arise from atoms moving at non-zero velocities such that the pump is in resonance with one transition and the probe is in resonance with the other transition.

Fig. 7: Electronic Controller

Frequency Sweep Calibration

In order to make quantitative measurements of the hyperfine splittings and compare these measurements to the handbook data, it is essential to calibrate the frequency sweep of the laser. This is accomplished with an unequal-arm Michelson interferometer shown as part of Figure 5.

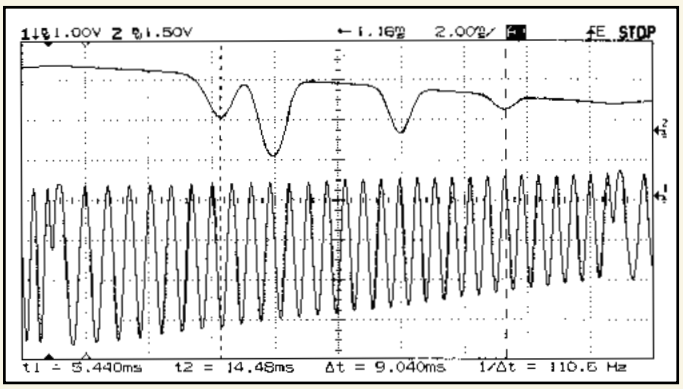

Fig. 9: Transmission Data with Interferometric Fringes

Straightforward measurement of the pathlength difference, $\Delta L = L_1 - L_2$, can be used to calibrate the frequency sweep in Hz/fringe. The optical frequency difference, δf, between two successive maxima will be $\delta f = c/2\Delta L$. For our layout, where ΔL = 0.35 meters, the sweep calibration is .429 GHz/fringe. The difference between the marked features of Figure 9 is then 6.65 ± 0.2 GHz. The accepted value is 6.835 GHz.

Resonant Absorption and Refractive Index

The relationship between the absorption and refractive index of rubidium gas, the Kramers-Kronig equation, can be studied as a function of temperature. While the absorption is easy to observe, the small changes in refractive index must be measured interferometrically. Although the mass density of the gas is extremely small, the effect is greatly enhanced by the S→P resonance where these measurements are made.

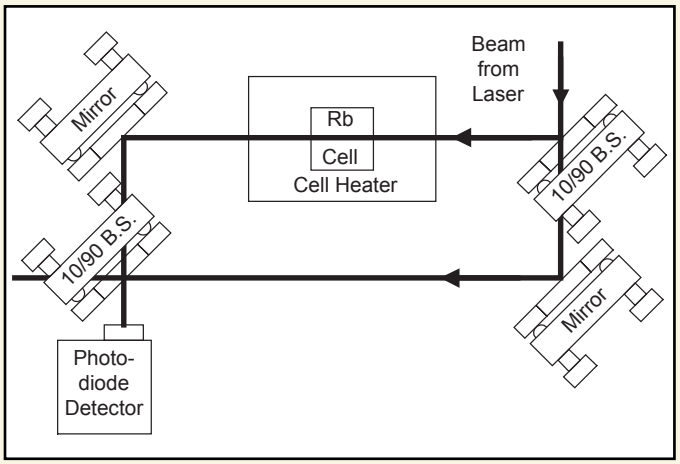

Fig. 10: Mach-Zehnder Interferometer Block Diagram

The experimental setup is shown in Figure 10. The Mach-Zehnder interferometer is used to measure the refractive index. Here, the input laser light is first split by a beamsplitter, and the beams travel down different paths through the interferometer. They are then recombined at a second beamsplitter. The intensity at the photodiode is sensitive to the relative phase of the two beams as they interfere at the second splitter.

The interferometric data and the calculated theoretical curves are shown in Figure 11.

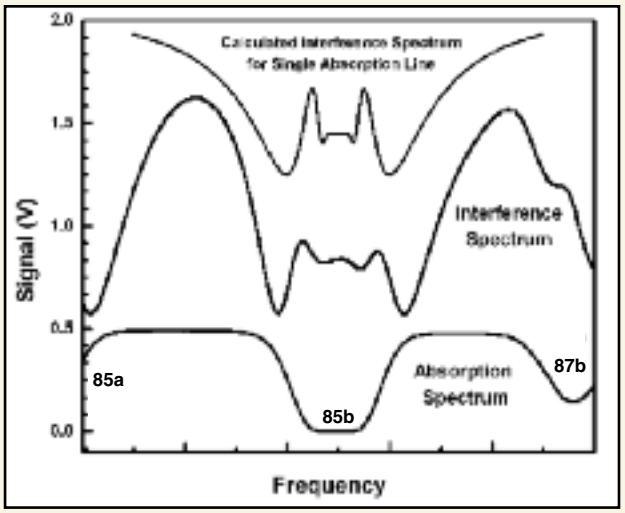

Fig. 11: Interferometric Data

Resonant Faraday Rotation

Those students familiar with the small magnitude of the Faraday rotation in bulk condensed matter might assume it would be impossible to detect the effect in a much more dilute gas sample. The following experiments with rubidium gas will surprise, maybe even amaze, them. The reason for this large effect is the enormous enhancement of both the rubidium absorption and dispersion responses that occur near the atomic resonance D_2 line at 780 nm.

Professor David Van Baak, another of TeachSpin's collaborating scientists, has published (AJP **64** 6) a detailed theoretical explanation of this Faraday rotation experiment. His simplified theoretical model of the atomic-light interaction is accessible to advanced undergraduate majors. The complete instrument includes all the essential components necessary to perform these measurements. Figure 12 is a block diagram of the apparatus.

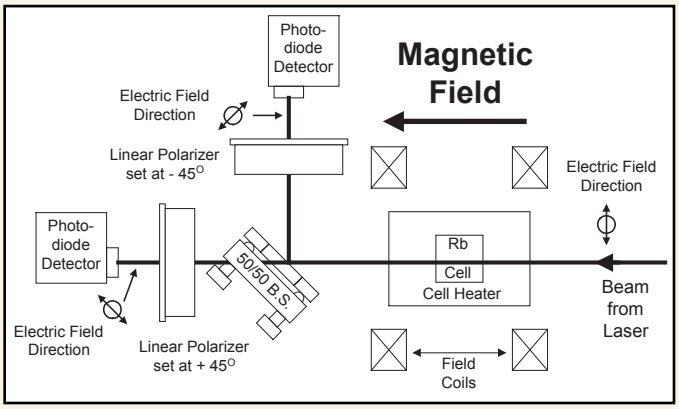

Fig. 12: Block Diagram, Faraday Rotation

Below, Figure 13 shows the experimental data as well as the theoretical predictions using Van Baak's model.

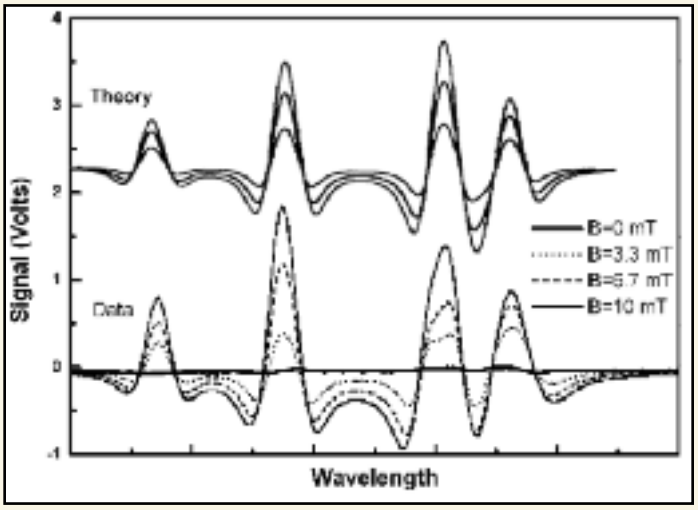

Fig. 13: Experimental and Theoretical Predictions

Zeeman Splitting

The magnetic field is used to resolve the Zeeman splitting of one of the Doppler-free transitions with the same setup (Figure 5), but using circularly polarized pump and probe light. The splitting observed is the sum of the splitting in the excited and ground states. The inset in Figure 14 shows the D-F spectrum from Rb D_1 line at 795 nm. The spectrum of the ^{87}Rb, F=2→F′ =1 transition for different magnetic field values is also shown. This line was chosen because it is well separated from other absorptions, allowing for uncomplicated observation of the Zeeman splitting.

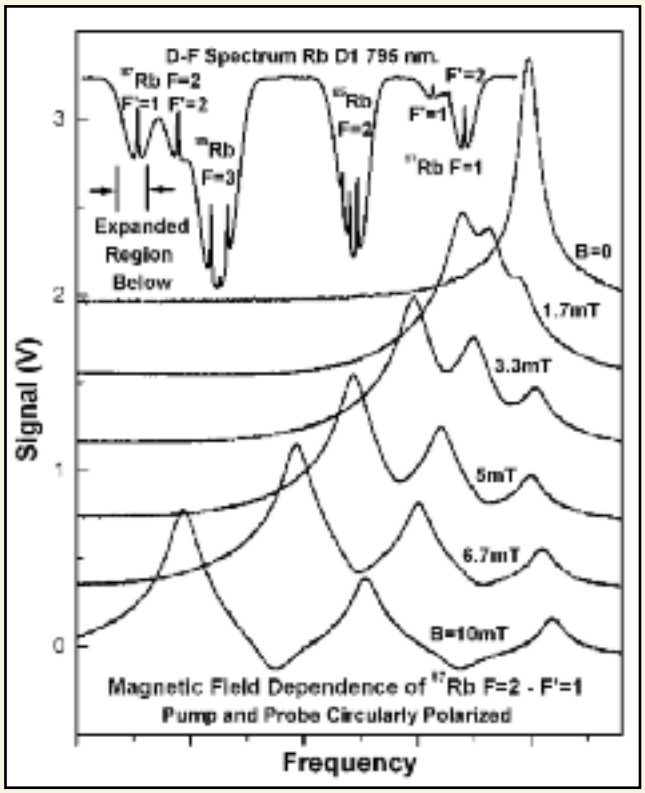

Fig. 14: Zeeman Splitting

SPECIFICATIONS

Laser Head
- Sanyo DL 7140-201 Max Power 70 mW
- Wavelength range: 15 nm coarse, 10 GHz fine,
- Temp. Range: 0 – 60°C

Controller Electronics
- Current: 0– 100 mA, Noise < 0.5 µA rms
- Piezo modulation: 0 – 100 V
- Ramp Gen: 1 mHz – 10 kHz, 0 – 10 V_{p-p}
- Cell Temp. Controller: Room – 100 °C
- Detector: Balance, Differential Gain 1– 100

Detectors
- Pin Photodiodes ¼" diameter
- I – V Preamp: 333 Ω – 10 MΩ in 1, 3, 10 Step

Rubidium Vapor Cell Module
- Helmholtz Coils: 10 mT @ 3 A
- Non-Magnetic Heater to 100°C
- Rubidium Cell: 1" Diameter x 1" Long

Optics (see price list for details)
- Mirrors, ND filters, Wedges, Beam Splitters, Polarizers

Included Accessories
- CCD Camera, 5" B&W TV Monitor, IR Viewing Card
- Optical Breadboard: 24" x 36" x ½", Black Anodized Al.
- 2 Pair Safety Goggles, Specialized Tools,
- Student/Instructor Manual

TEACHSPIN, INC.
2495 Main Street, Suite 409, Buffalo NY 14214-2153
Phone/Fax 716-885-4701 www.teachspin.com